In Vivo Evaluation of Nerve Guidance Conduits Comprised of a Salicylic Acid-based Poly(anhydride-ester) Blend

by

YONG SOO LEE

A thesis submitted to the

Graduate School-New Brunswick

Rutgers, The State University of New Jersey

And

The Graduate School of Biomedical Science

University of Medicine and Dentistry of New Jersey

in partial fulfillment of the requirements

for the degree of

Master of Science

Graduate Program in Biomedical Engineering

written under the direction of

Kathryn E. Uhrich

and approved by

_____

_____

_____

New Brunswick, New Jersey

October 2012

ABSTRACT OF THE THESIS

In Vivo Evaluation of Nerve Guidance Conduits Comprised of a Salicylic Acid-based Poly(anhydride-ester) Blend

By Yong Soo Lee

Thesis Director:
Kathryn E. Uhrich

Unlike the central nervous system, peripheral nervous system can regenerate from injury. However, without surgical intervention, the results are often poor. Autologous nerve grafting is the golden standard for repairing peripheral nerve injury; but limited donor availability and donor site morbidity led researchers to seek alternative methods. Among the many alternative treatment options, synthetic nerve guidance conduits (NGCs) have been most actively developed. The goal of NGCs is to serve as a physical scaffold that aids the axonal regeneration process while preventing scar tissue formation that interferes with regeneration. Biocompatible and biodegradable NGCs would provide additional benefits: minimize foreign body reaction and avoid secondary surgeries to remove NGCs. We developed a unique NGC that incorporated the characteristics described above and can release an anti-inflammatory drug, salicylic acid. In this work, *in vivo* assays were performed to evaluate NGCs fabricated from a poly(anhydride-ester) blend. To further assist in the regeneration process, bovine native collagen type I hydrogel were inserted into the NGCs lumen which was then implanted in femoral nerve of mice for up to 16 weeks. These studies demonstrated *in vivo* biodegradability, biocompatibility, and axonal regeneration following an injury to the peripheral nerve. These studies provide greater

insights into the importance of designing NGCs and how they aid in regeneration and functional recovery of subjects.

DEDICATION

To my loving parents, who have constantly supported, trusted and kept me in their prayers up until this point and will continue to do so.

ACKNOWLEDGEMENTS

I would like to express my utmost gratitude towards to all those that guided, collaborated with and trained me to present the research work here in this thesis.

With Special Thanks to:

Dr. Kathryn E. Uhrich, Dr. David I. Shreiber, Dr. Li Cai, Dr. Jeremy Griffin, Dr. Jian Chen, Dr. Ijaz Ahmed, Dr. Roberto Delgado-Rivera, Dr. Dawanne Poree, Dr. Bryan Langowski, Dr. Adam York, Dr. Sarah Hehir, Dr. Andrew Voyiadjis, Dr. Isaac Kim, Dr. Gary Monterio, Sabrina Snyder, Reselin Rosario-Melendez, Denise Cullerton, Allison Faig, Li Gu, Kevin Memoli, Michelle Ouimet, Nicholas Stebbins, Weiling Yu, David Orban, Pancrazio Papapietro, Sammy Gulrajani, Kristina Wetter, past and present members of Uhrich group, Shirley Masand, Ian Gaudet, Aaron Carlson, Jeffrey Barminko, David Xu Dong, Hsuan Yu Shih, Andrea Gray, Ana Rodriguez, Alex Brunfeldt, Vasilis Niotis, Gabriel Yarmush, Mehdi Ghodbane, Michael Koucky, Najeeb Chowdhury, Edek Williams, Emmanuel Ekwueme, Brittany Taylor, Jocie Cherry, Serom Lee, Jennifer Kim, Ka Po Chu, Jean Lo, Sagar Singh, Joe Kim, Isaac Perron, Justin Satter, Leora Nusblat, Lawrence Sasso, Bekah Gensure, Mohammad Zia, Mohammad Sadik, Linda Johnson, Lawrence Stromberg, Rutgers BESS, Sanghwan Park, Hyungsub Shim, Eunhee Park, Haewon Yoon, Byungjoo Park, Jinwook Lee, Seungkyoo Lee, Kyungjae Lee, Youngho Kim, Jongpil Kim, Bioabsorbable Therapeutics Inc, US Army contract # W81XWH-04-2-0031, and faculty and staff of Rutgers-UMDNJ Biomedical Engineering, and Rutgers University.

Please forgive me if I have neglected to include you in the list.
I could not have done without the support from people who care for me.

TABLE OF CONTENTS

LIST OF TABLES

LIST OF FIGURES

LIST OF EQUATIONS

1. INTRODUCTION

1.1. Peripheral nerve injury

In an epidemiology study conducted at a level I trauma center in Ontario, about 2.8% of patients admitted suffered from peripheral nerve injury (PNI).[1] Another study revealed that in western societies, about 660,000 patients suffered from PNI annually, with trauma being the leading cause.[2,3] PNI patients may suffer from loss of sensation, severe pain, paralyzed muscles and loss of function, affecting the quality of life.[4] In addition to diminished quality of life, PNI patients are faced with economic hardship arising from longer time out of work and high cost of healthcare associated with treating PNI.[4,5]

1.2.Peripheral nerve

The peripheral nervous system (PNS) is primarily composed of neurons, Schwann cells, and connective tissues and blood vessels.[6] Schwann cells form myelin sheaths around axons serving as an insulator for electrical signal to ensure fast conduction velocity (up to 100 m/s). Axons and Schwann cells together form nerve fibers that can transmit electrical signal from one part of the body to another.[6,7] Without proper myelination, nerve fibers transmit electrical signals at a slower conduction velocity (<1m/s).[6]

1.3. Regeneration process

The PNS is capable of axonal regeneration when the size of lesion is < 5 mm gap for adults in humans.[8] Following a nerve injury, the nerve fiber distal to injury site begins to degenerate marking the beginning of Wallerian degeneration.[9,10] Wallerian degeneration is a sequence of events occurring distal to nerve lesion following a nerve injury.[11] Wallerian degeneration may not begin until few days after injury for humans

and 24~48hr following injury for mice and rats.[12] During the initial phase of Wallerian degeneration, the cytoskeletal networks within the axons break down, causing the damaged axons to become fragmented (**Figure 1**).[2] Schwann cells also contribute to

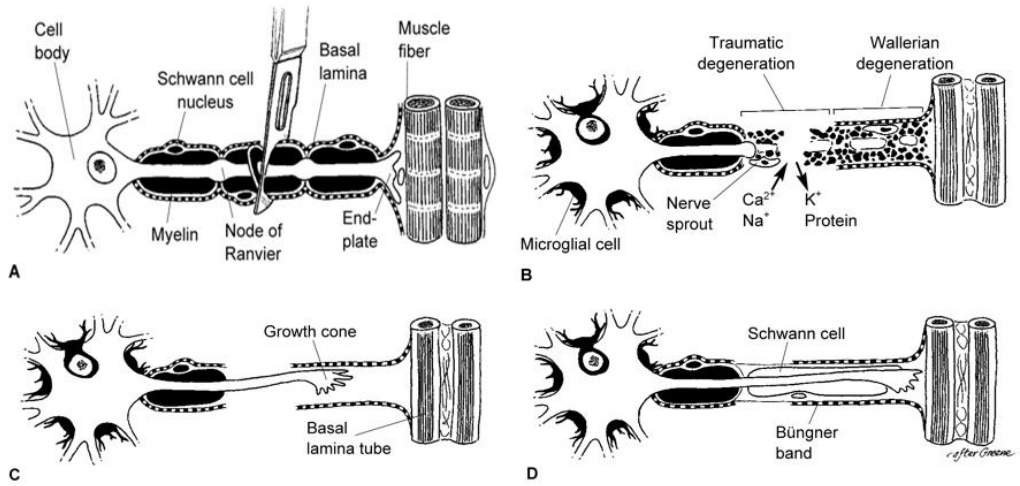

degeneration by fragmenting myelin sheath that surrounds axons.[2]

Figure 1[13]. Degeneration and regeneration of the peripheral nerve: (A) Axonal injury; (B) Traumatic degeneration and Wallerian degeneration; (C) Growth cone regeneration; (D) Bungner bands and Schwann cell. (Adapted from Seckel BR: Enhancement of peripheral nerve regeneration. Muscle Nerve 1990; 13: 785-800. Copyright 1989 Lahey Clinic. Reproduced with permission from John Wiley & Sons, Inc.)

Schwann cells then dedifferentiate, removing myelin debris while proliferating and forming the bands of Bungner which guide and support regenerating axons from the proximal to distal nerve stumps (**Figure 1**).[9,11,14,15] Macrophages recruited to the injury site also contribute to the removal of myelin debris.[2,9] Fibrin matrix proteins originating from plasma also enter the injury site to bridge the gap between the nerve stumps and allow migration of fibroblasts, Schwann cells, and other endothelial cells.[16] Within a few days, fibrin is replaced by collagen fibers and other extra cellular matrix (ECM) , which guide growth cones of regenerating axons.[17] Current treatments, as outlined below, attempt to utilize this regeneration process by providing structural support that will direct migrating Schwann cells and regenerating axons to the distal stump.

2. TREATMENT OF PNI

2.1. Traditional treatment options: Surgery and grafts

The majority of treatments for PNI include suturing the nerve ends for short gaps and grafting autologous nerves at the injury site.[9,18,19] Despite the potential for axonal regeneration, current treatment are limited as they do not guarantee functional recovery and cannot be used for all of peripheral motor nerve injury from accidents and traumas as detailed herein.[8] End-to-end nerve suturing is limited to short gaps and introduces tension at the operation site leading to a painful sensation for patients.[20,21] Autologous grafts, the gold standard of treatment options for PNI, is often limited by the availability of donor nerves that can be harvested, potential mismatches in size, formation of neuromas (thickening of nerve fibers leading to formation of a bulb), as well as loss of sensory function at the donor site.[8,22,23,24] Although results are often successful, the collective drawbacks of autologous grafts have motivated the need for synthetically fabricated nerve guidance conduits (NGCs) for nerve repair.

2.2. Synthetic NGCs

Like autologous grafts, NGCs serve as a matrix bridging the gap of severed nerves and preventing fibroblast influx, thereby preventing scar tissue formation that competitively occurs with axonal regeneration and leading to possible neuroma formation.[8,24-26] Synthetic NGCs can treat small lesions of PNI and should be biocompatible to reduce foreign body reactions that may interfere with the regeneration process. Initially, non-degradable synthetic NGCs such as inert and biocompatible polyethylene (PE) and silicone tubes were used to minimize foreign body reaction.[25,27] However, further studies demonstrated that as the regeneration of nerve tissues occurs, the nerve tissues were subject to constriction by the rigid non-

biodegradable NGC and caused chronic pain to impede functional recovery.[8,27] Eventually, these non-biodegradable NGCs needed to be removed, thus requiring a second surgery.[27] Therefore, scientists began to develop *biodegradable* NGCs to prevent constriction and obviate the need to remove the NGCs.[27] In addition to biocompatibility and biodegradability, many physical factors must be considered when designing NGCs such as batch-to-batch variability, porosity, permeability, swelling, and flexibility.[27,28] NGCs derived from biological sources such as collagen, provide structural support for the axon regeneration, but raise concerns regarding batch-to-batch variability, thus, NGCs fabricated from synthetic sources may be a better alternative.[29] Porosity and pore size must be within a certain range to prevent cell infiltration of cells that may hamper axon extension while allowing the exchange of waste materials, nutrients and blood vessel infiltration.[8,28] Permeability controls the pressure within the NGCs through exchange of fluid and gas. It also influences fibrin cable formation during the initial phase of nerve regeneration.[25,28,30] Swelling of the NGCs may occlude the lumen and inhibit the regeneration process or compress the regenerated nerve, as observed with non-degradable NGCs.[28,31] The degradation rate plays an important role during and after regeneration. If degradation occurs too rapidly, the NGCs will collapse prior to full axonal regeneration, leading to poor recovery because of limited mechanical stability.[28,31] Slow degrading NGCs will behave like non-degradable NGCs, causing constriction on regenerated axons leading to pain.[28] Flexible NGCs can be used for larger nerve gap repairs where the transected nerve ends not line up or may need to bridge across a joint.[28]

A successful synthetic NGC for treating PNI that leads to functional recovery must fulfill two vital criteria: containing growth-supporting cues and providing physical support.[23, 25] Growth factors and other biochemical molecules can be

incorporated into NGCs in the form of microspheres or embedded in luminal fillers that may further aid the axonal regeneration process.[28] In addition to growth factors and biochemical molecules, cellular components such as Schwan cells and mesenchymal stem cells can be incorporated into NGCs to create a favorable microenvironment.[25]

Several polymer-based synthetic NGCs are under investigation that can meet the physical requirements of NGCs. Poly(lactide acid) (PLA), poly(glycolic acid) (PGA), poly(lactide-*co*-glycolide) (PLGA), and polycaprolactone (PCL) are some of commonly used materials for fabricating NGCs.[8] In addition to being biocompatible and biodegradable, the degradation rate and mechanical properties of these polymers can easily be tailored.[8] However, NGCs fabricated from these polymers have potentially adverse effects *in vivo* due to acidic byproducts of degradation, which can negatively affect functional recovery and reduce axonal growth.[8,22] PLGA NGCs also tend to collapse *in vivo* due to poor mechanical strength.[8] In addition to reduced functional recovery, synthetic NGCs can also elicit an adverse immunological response such as swelling at the implantation site due to the high concentration of degraded polymer.[32] To avoid these known problems, polyanhydride-based scaffolds are being studied.[33]

2.3. Salicylic acid-based poly(anhydride-esters) (PAEs)

Salicylic acid-based poly(anhydride-esters) (PAEs) contain two different types of hydrolytically cleavable bonds in their polymer backbone.[34] Combined with surface erosion degradation and pH-dependent hydrolytic bond cleavage, PAEs release water-soluble, biocompatible byproducts and salicylic acid, a non-steroidal anti-inflammation drug (NSAID) **(Figure 2)**.[35,36]

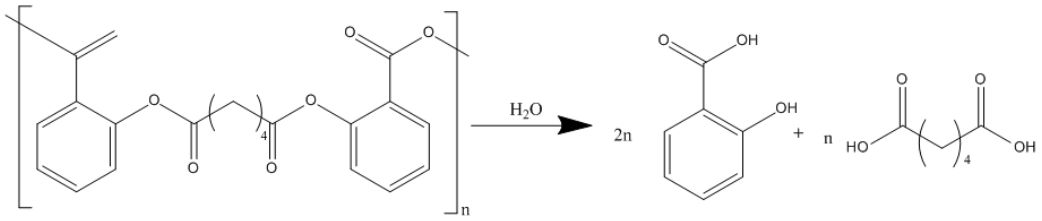

Figure 2. Chemical structure of a salicylic acid-based poly (anhydride-ester) with *n* repeating units and its degradation products.

PAEs have high drug loading capacity and drug release rates that can be controlled via a biocompatible linker.[37] In addition, PAEs have glass transition temperatures (T_g) above physiological temperature that will prevent loss of mechanical integrity when placed in the body.[38] These excellent thermal and mechanical properties allow fabrication of various biomedical devices including from films, disks, microspheres, fibers and NGCs.[39]

2.3.1. Drug-releasing NGCs

When designing NGCs, it must meet the physical requirements previously discussed previously and preferably provide factors to promote axonal recovery. In previous studies, a PAE was prepared that chemically incorporated salicylic acid and blended with poly(lactide acid anhydride) (PLAA) to fabricate NGCs.[38]

The degradation products of the PAE (i.e., salicylic acid) compares favorably to other synthetically fabricated NGCs that release biochemical agents that exacerbate local inflammation.[8,22] Local release of salicylic acid from the PAE NGCs has the additional benefit of inhibiting a cascade of inflammatory responses such as swelling and infection without relying upon systemic NSAID therapy.[35] Localized drug delivery can potentially achieve greater tissue-level concentrations at the target site relative to systemic treatments.[40] In addition to achieving greater potency, local drug delivery minimizes toxicity as compared to systematic drug delivery.[40]

2.4. Native collagen fillers

Although synthetic NGCs demonstrate nerve regeneration across short lesion gaps, regeneration in long lesions is often not successful because of the inability to form complete fibrin cables.[25] Incomplete formation of ECM and fibrin cables prevents cell migration from nerve stumps, leading to poorly regenerated nerves.[17] To promote regeneration, biochemical factors such as cells, neurotropic factors and ECM are also required.[8] Studies have shown that using collagen hydrogels as fillers for NGCs provides a growth medium for regenerating nerves.[8,17,18,25,41] Collagen fillers increase myelinated fibers and demonstrate superior electrophysiological responses when compared to hollow NGCs.[17,18,26,41,42] Matrix components may also provide a substrate for the binding of neurotropic factors, which facilitates the early ingrowth of both neural and non-neural cells.[28]

2.5. Goals of PAE NGCs

In this study, biodegradable NGCs synthesized from salicylic acid-based PAE and PLAA blends were used to test the functional recovery of mice following PNI. During the course of recovery, the polymer-based NGCs were expected to degrade and release salicylic acid. To further assist the functional recovery, NGCs were filled with native collagen.

3. METHODS AND MATERIALS

3.1. *In vivo* evaluation

3.1.1. Preparation of NGCs

PAE NGCs were fabricated by Dr. Jeremy Griffin, as previously described.[38,43] Two ends of the polymer conduits were drilled to make the suture holes prior to the animal surgery. In brief, using an optical dissection microscope (Reichert Inc.,

Buffalo, NY) and 30 gauge needles, holes were drilled while holding one end of NGCs with the coarse forceps.

3.1.2 Sterilization of NGCs

Prior to surgery, all PAE-based NGCs were sterilized using UV light (λ= 254 nm) prior to filling NGCs with saline and/or native collagen. NGCs were left in a UV chamber (Spectrolinker 1500XL, Spectroline) for 15 min, rotated, and sterilized for another 15 min. Following sterilization, NGCs were taken to the laminar flow hood immediately and submerged in 70% aqueous ethanol for 10 min. After 10 min, the 70 % aqueous ethanol was vacuumed off and the NGCs were rinsed with sterile phosphate buffered saline (PBS) (Sigma) three times.

3.1.3. Collagen-hydrogel fillers

Native collagen hydrogels at 2.0 mg/mL were prepared by Shirley Masand (Dr, Shreiber's lab, Rutgers BME) based on previously published protocols.[44] In brief, fetal calf type I collagen (EPC) was reconstituted to 3 mg/ml in 0.02 N acetic acid (Sigma) to make an oligomeric collagen solution. The solution was neutralized using 1M Hepes 2 % (Fluka), 0.1 N NaOH 14 % (Sigma), 10X minimum essential medium 10 % (Sigma), M199 5.2 % (Sigma), penicillin/streptomycin 0.1 % (Sigma) and L-glutamine 1 % (Sigma).[44,45] To allow self-assembly of collagen hydrogels, the solution was added to a microtiter plate and incubated at 37℃ for 30 minutes. Using an insulin needle (BD), excess collagen hydrogel or PBS was injected into NGCs or polyethylene tubes (BD).

3.1.4. Animal surgery

All animal surgeries were performed by Dr. Jian Chen (Rutgers, W.M. Keck Center for Collaborative Neuroscience) and complied with the university standard protocols for animal handling and care. The animals were anesthetized by

intraperitoneal injections of ketamine (80 mg/kg) (Butler Schein) and xylazine (12 mg/mg) (Butler Schein). Maintaining sterile conditions, as mean of preventative anesthetic, bupivaccine (0.1 mg of 2.5% solution) (Butler Schein) was subcutaneously injected at the incision site of left hind limb, which was first shaved and wiped down with betadine (Butler Schein). The nerve transection was performed at a 3 mm distance proximal to the bifurcation of the nerve upon exposing the left femoral nerve. The cut ends of the nerve were inserted into a polyethylene tubing (PE) (BD) with dimension of 3 mm in length and 0.38 mm inner diameter) or PAE NGCs where polyethylene tubing served as a control group. Both PE and PAE NGCs were fixed with single epineural 11-0 nylon stitches to allow a 2-mm gap between the proximal and distal stump and the skin wound was closed with 6-0 sutures (Ethicon). The femoral nerve model was chosen to study the peripheral nerve regeneration as it allows studies on mechanism of determining the molecular sensitivity of reinnervation.[46]

3.1.5. Video recording and measurement: Classical beam walk test

Female C57BL/6J mice were obtained from Charles River Laboratory (North Franklin, CT) at the age of three months. Prior to carrying out *in vivo* evaluation of NGCs, mice were trained to perform a classical beam walk test.[46] Individual mice placed on one end of the beam walked to the other end of the beam where a cage was placed.[46] The caging serves as incentives for mice to walk on the wooden beam (1000 mm in length, and 38 mm in width).[46] Mice were continuously trained from three trials to five or more runs over two weeks until they walked on a beam in a continuous fashion without frequent stopping. For duration of 16 weeks, the gait movement of mice was recorded using a high-speed camera (A602fc, Basler, Ahrensburg, Germany). The camera was positioned such that a rear view of the mice

walking on the beam was recorded. For all mice, recorded videos were saved on a personal desktop computer in Audio Video Interleaved (AVI) format. Video recordings done prior to animal surgery are set as week 0. Weeks 0, 1-4, 6, 8, 10, 14, and 15 were recorded to film the gait movements of mice. Using SIMI Motion 7 software (SIMI Reality Motion Systems, Unterschleissheim, Germany), single frames corresponding to the gait movement of the left hind limb were used to measure the foot-base (FBA) angles.

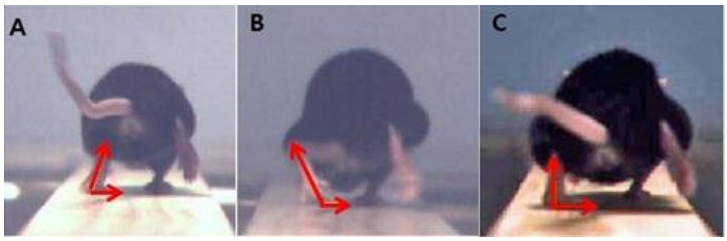

Figure 3. Classical beam walk test: (A) Gait movement of mice prior to surgery; (B) gait movement one week after the injury; (C) and gait movement at the 15 week of study. Red arrows depict the foot base angle (FBA).

At toe-off position, the angle between a line drawn dividing the sole surface into two halves and a horizontal line defines the FBA; this measurement is in respect to medial position (shown as red arrows on **Figure 3).** Knee joint extension during gait movement is dependent on the quadriceps muscle which is innervated by the motor branch of femoral nerve and can be refelcted by FBA measurements. [47] Measurement of functional recovery at various time points can be obtained using stance recovery index (RI) calculated using following equation:

Equation 1. $RI=[(X_{reinn}-X_{den})/(X_{pre}-X_{den})] \times 100$

where X_{reinn}, X_{den} and X_{pre} are values obtained during the period of reinnervation (reinn), during the state of denervation (7 days after injury) (den), and prior to nerve injury (pre), respectively.[47]

3.1.6. Video recording and measurements: Pencil grip test

Voluntary pursuit movement of the mice yields a limb protraction length ratio (PLR); this measurement was recorded and analyzed using single frame motion capture. Because this study involves involuntary motion, training of mice was not necessary.

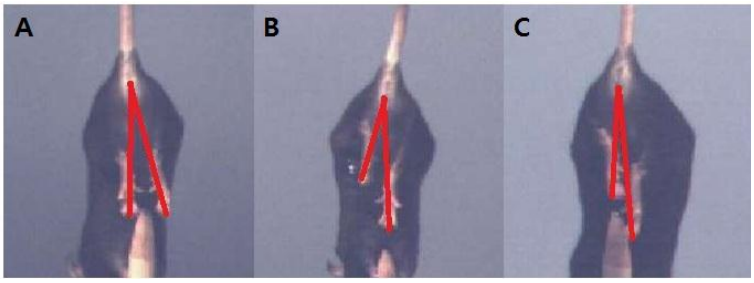

Figure 4. Pencil grip test of mice: (A) Protraction of hind limbs prior to surgery; (B) protraction of hind limbs one week following surgery; and (C) protraction of hind limbs at 15 week of study. Red lines depict the relative length of hind limbs lengths. Note that the pencil is shown at bottom of photos.

Held by its tail and lowered towards a stationary pencil, the mouse holds onto the pencil and extends both hind paws towards the stationary pencil.[46] Mice were filmed at weeks 0-4, 6, 8, 10, 12, 14, and 15. The relative length of the two hind paws are estimated by lines connecting the distal midpoint of hind paws to the anus **(Figure 4)** using SIMI Motion 7 software (SIMI Reality Motion Systems, Unterschleissheim, Germany). The ratio of the right to left limb length was measured prior to surgery, 7 days following surgery, and during the course of nerve regeneration as shown in **Figure 4**. Measurement of functional recovery at various time points can be obtained using stance recovery index (RI) calculated using **Equation 1.**

3.2. Histology

3.2.1. Animal sacrifice

All animal sacrifices were performed by Dr. Jian Chen (Rutgers, W.M. Keck Center for Collaborative Neuroscience) and complied with the university standard protocols for animal handling and care. Mice were deeply anaesthetized using

intraperitoneal injection (IP) of a combination of ketamine (80mg/kg) (Butler Schein) and xylazine (12mg/kg) (Butler Schein) then perfused transcardially with physiological saline followed by 4% formaldehyde in 0.1M sodium cacodylate buffer at pH 7.3. For histological studies, the left femoral nerve was cut at a distance of approximately 3 mm distal from the bifurcation of nerve into motor and sensory branches. The left femoral nerve and muscle tissues were collected and postfixed overnight in 4% formaldehyde at 4 ℃ then immersed in 20 % solution of sucrose in DI water for storage prior to analysis.

3.2.2. Sample preparation

Prior to sectioning, all tissues were processed in epoxy resin which was carried out by Dr. Ijaz Ahmed (Dr. Shreiber research lab Rutgers). All tissues were fixed in 4 % paraformaldehyde (Sigma) in 0.1 M phosphate buffer (Sigma) overnight, then washed twice in 0.1M phosphate buffer two times for 1 hour at 4 ° C. After washing, the samples were post fixed in 1 % osmium tetroxide (OsO_4) (Electron Microscopy Sciences) in 0.1 M phosphate buffer for 1 hour. OsO_4 solution (1%) was prepared by mixing equal quantities of 2 % aqueous OsO_4 and 0.2 M phosphate buffer. Fixed samples were then rinsed twice in 0.1 M phosphate buffer for 5 minutes. Dehydration was done in 50 % ethanol for 10 minutes followed by dehydration in 70 % aqueous ethanol for 20 minutes. Samples were again dehydrated twice in 90 % aqueous ethanol for 10 minutes then dehydrated in 95 % aqueous ethanol for 10 minutes. The last step of dehydration was done using 100 % aqueous ethanol for 20 minutes which was repeated twice.

Upon finishing the dehydration, the samples were immersed in propylene oxide (Electron Microscopy Sciences) for 10 minutes and repeated twice. Propylene oxide and epoxy resin (Electron Microscopy Sciences) mixtures were made at 75/25 ratio in

which samples were placed for 1 hour. Samples were then placed in 50/50 mixture of propylene oxide/epoxy resin for another hour. Samples were subsequently placed in 25/75 mixture of propylene oxide/epoxy resin for another hour. Samples were placed in vials and left uncapped overnight to evaporate the propylene oxide. Samples were removed from vials and embedded in rubber molds with freshly prepared resin which was polymerized at 60 ℃ for 24 hours.

Prepared resins were sectioned at approximately 1 μm thick using glass knives on an unltramicrotome (Cryotome Electronic cryostat). Sectioned samples were dried onto a glass slide on a hotplate at 80℃. Sections were stained with 1% toluidine blue (used as contrast agent) in 1% borax solution (Electron Microscopy Sciences) for 1 minute at 80C°. With distilled water, stains were rinsed off from the samples then subsequently air dried and covered with a glass coverslip using a synthetic mounting medium such as D.P.X (Distrene, Plasticiser, Xylene (Electron Microscopy Sciences)).

3.2.3. Microscope imaging

An inverted confocal optical microscope, Olympus IX81 (Olympus), was used to image the transverse cross section of the femoral nerve. MetaMorph microscopy software was used for imaging slides using the 20X and 100 X oil objectives. Because the sections were 1 μm thick and prepared from sections distal to the bifurcation branches of the motor and sensory nerves, all samples contained identical structures. The 4X objective lens was used to identify samples with minimal processing damage such as bubbles or loss of tissue connectivity. When using 100 X oil objective lens, the images were overlapped and contained corners to ensure that proper mosaic images can be made for later analysis. Using Microsoft ICE software, images were stitched together to form a complete mosaic picture.

3.3. Image analysis

3.3.1. Axon counts

To count the number of myelinated axons, images taken at 100 X were analyzed using Image J software. Myelinated axons were identified by the presence of a thick black halo surrounding a white circular axon as shown in **Figure 5A.** Some myelinated axons, known as Schmidt-Lanterman incisures, are surrounded by Schwann cells indicating the on-going process of myelination (**Figure 5B).**[48]

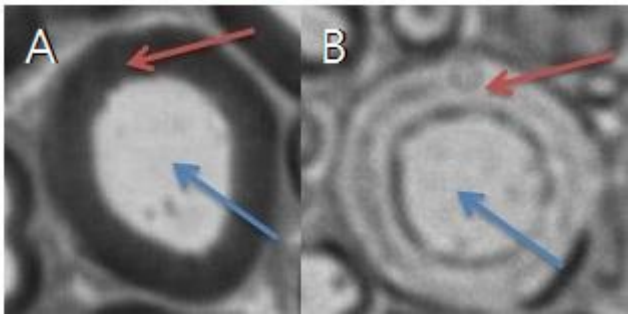

Figure 5. Myelinated axons: (A) Myelinated axon where red arrow highlights the myelin stained with OsO_4 while blue arrow shows the axon; (B) Schmidt-Lanterman incisures where red arrow shows the Schwann cell wrapping around the axon (blue arrow).

For the g-ratio calculation (**see section 3.3.2. Regeneration degree**

In a healthy nerve, myelinated axons are tightly packed within the nerve. Upon injury, myelinated axons are degraded by the Wallerian degeneration process then are regenerated and remyelinated during the recovery period. **Figure 6a** shows a physiologically healthy nerve that is filled with myelinated axons while **Figure 6b** shows partially regenerated nerve and **Figure 6c** shows poorly regenerated nerve. Degree of regeneration is a method to quantify the degree of regenerated axons and can be calculated by dividing the area of remyelinated axons by the total area of the nerve as shown in **Figure 7**.

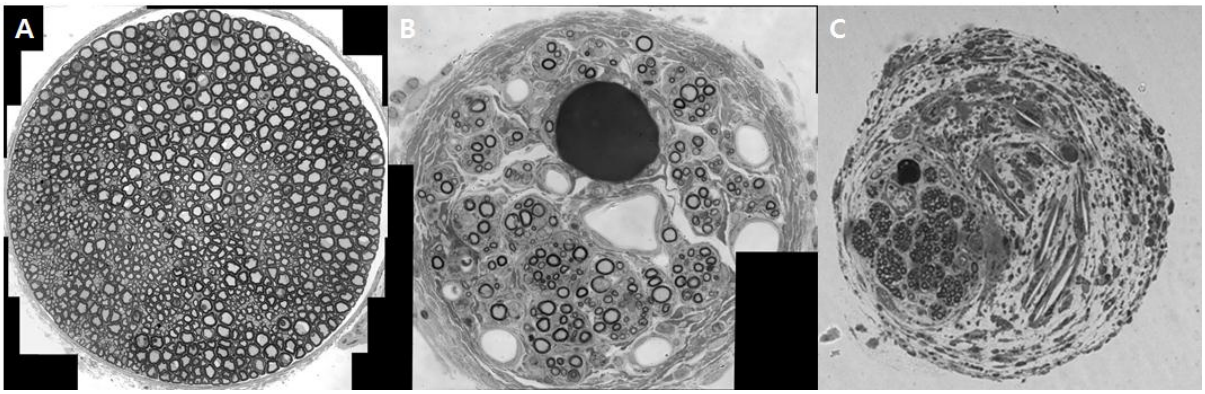

Figure 6. Cross-section of peripheral nerves: (A) Healthy nerve tightly packed with myelinated axons; (B) Partially regenerated nerve; (C) Poorly regenerated nerve.

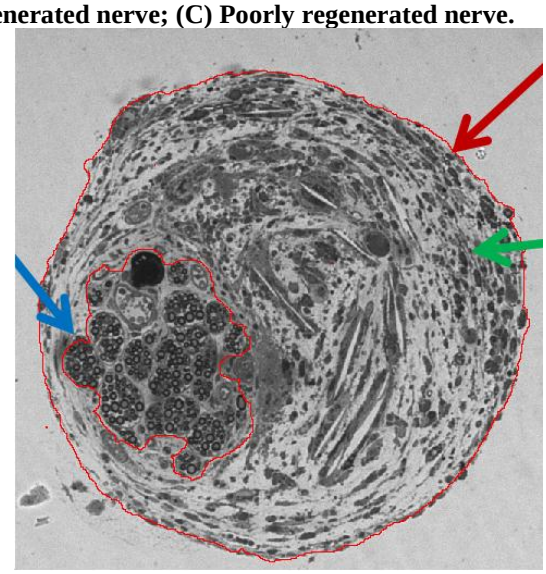

Figure 7. Cross-section of regenerated peripheral nerve. Red arrow highlights the total area of nerve while blue arrow shows remyelinated axons and green arrow shows scar tissues area

3.3.3. g-Ratio) (ratio of axon diameter to fiber diameter), Schmidt-Lanterman incisures were excluded from cell counts as they represented partial or incomplete myelination at the time of animal sacrifice.

3.3.2. Regeneration degree

In a healthy nerve, myelinated axons are tightly packed within the nerve. Upon injury, myelinated axons are degraded by the Wallerian degeneration process then are regenerated and remyelinated during the recovery period. **Figure 6a** shows a physiologically healthy nerve that is filled with myelinated axons while **Figure 6b** shows partially regenerated nerve and **Figure 6c** shows poorly regenerated nerve. Degree of regeneration is a method to quantify the degree of regenerated axons and

can be calculated by dividing the area of remyelinated axons by the total area of the nerve as shown in **Figure 7**.

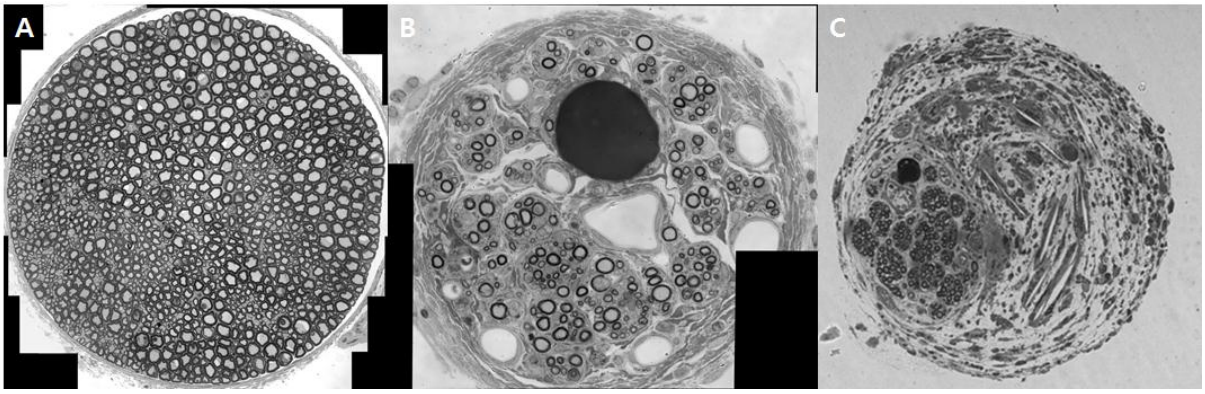

Figure 6. Cross-section of peripheral nerves: (A) Healthy nerve tightly packed with myelinated axons; (B) Partially regenerated nerve; (C) Poorly regenerated nerve.

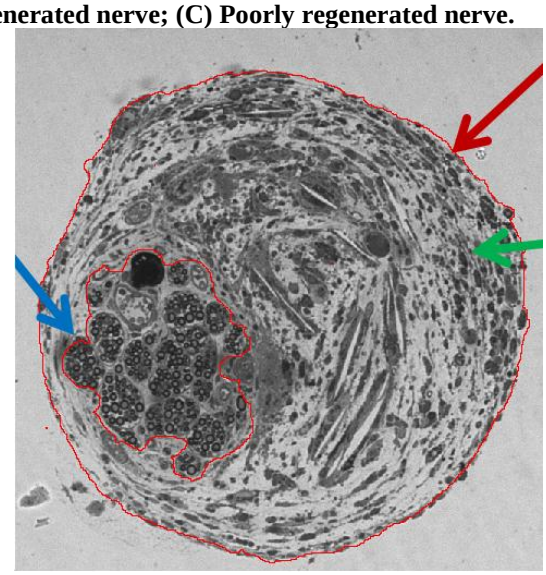

Figure 7. Cross-section of regenerated peripheral nerve. Red arrow highlights the total area of nerve while blue arrow shows remyelinated axons and green arrow shows scar tissues area

3.3.3. g-Ratio

Myelination can have a dramatic impact on the structure and physiology of an axon and surrounding tissue.[49] g-Ratio is widely used to assess the axonal myelination and the optimal g-ratio (varying values for different species, where 0.6~0.8 is optimal for mice) indicates maximal efficiency and physiological optimization.[49,50]

g-Ratio is calculated using **Equation 2**,

$$\textbf{Equation 2. g-Ratio=}\ \frac{\left(\frac{L1+L2}{2}\right)}{\left(\frac{D1+D2}{2}\right)}$$

where L_1 and L_2 (indicated in red arrows in **Figure 8**) are the lengths of the longest axis of the inner circle of the myelinated axon and the orthogonal length, whereas D_1 and D_2 (shown by blue arrows in **Figure 8)** are the lengths of the longest axis of outer circle of myelinated axon and the orthogonal length.

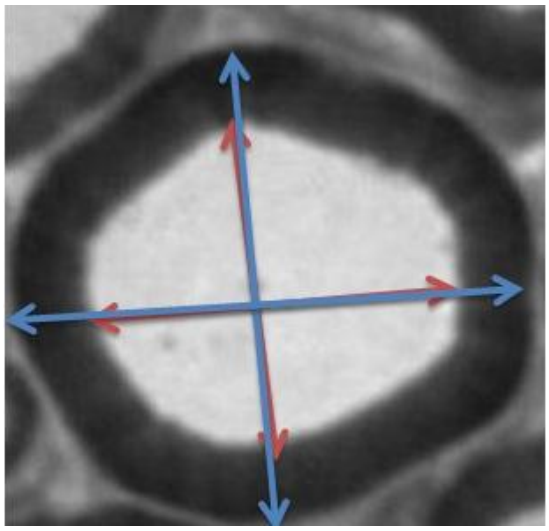

Figure 8. g-Ratio measurement of myelinated axon. Red arrows illustrate the mean diameter of axon (long and short axes) while blue arrows illustrate the mean diameter axon and myelin (long and short axes).

3.4. Statistical analysis

Both *in vivo* studies of beam walk and pencil grip were subjected to statistical analysis using Kalediagraph (http://www.synergy.com/company.htm). One-way analysis of variance (ANOVA) analysis and two-way ANOVA were performed to determine the statistical significance of various data sets where $p<0.05$ was considered significant.

4. RESULTS AND DISCUSSION

The femoral nerve was transected near the bifurcation points of the nerve into motor and sensory branches. The femoral nerve controls the quadriceps in mammals and during walking, the quadriceps support the swing of the contralateral legs and leads to abnormal walking in humans if the quadriceps are injured.[46] In mice, injury to

the quadriceps leads to impaired gait movements that can be easily measured and provide a reliable method to study peripheral nerve injury.

4.1. Functional recovery assessment: Classical beam walk test

Changes in gait movement can effectively evaluate regeneration due to implanted NGCs in a femoral nerve injury model. Abnormal gait movements produced by the impaired quadriceps was determined by measuring the foot base angle (FBA) using a single frame video analysis during the classical beam walk test.[46,47]

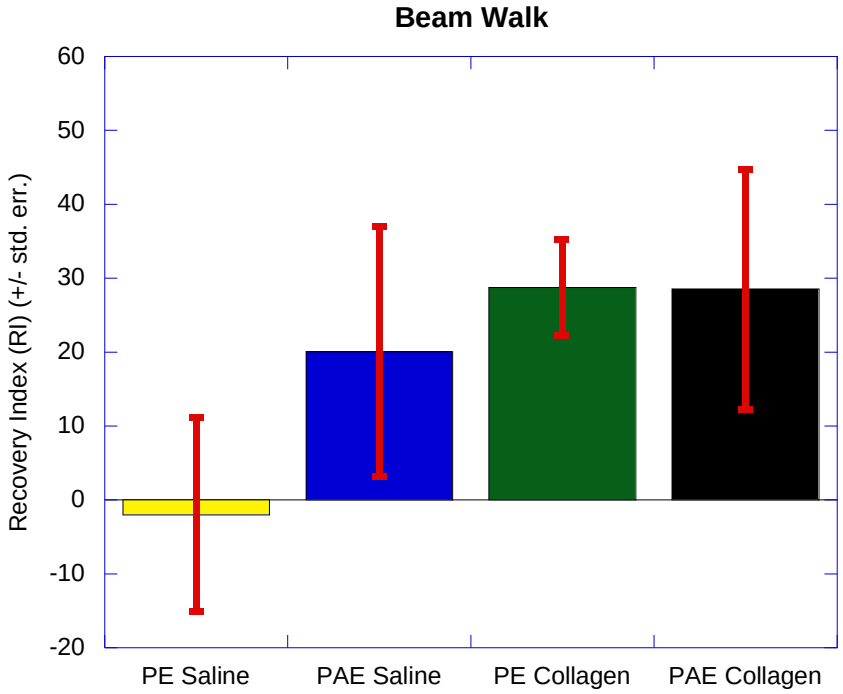

Figure 9. Classical beam walk test: functional recovery index of mice implanted with different NGCs filled with either saline or native collagen at 15 weeks post-surgery.

Figure 9 depicts the recovery index (RI) calculated for each test group 15 weeks post-surgery as measured by the classical beam walk test. A functional recovery of zero indicates that there was no improvement relative to 1 week post-surgery. All data in **Figure 9** was plotted as mean ± standard error. Negative functional recovery means that gait movement was further impaired relative to 1 week post-surgery. Positive functional recovery correlates to improved gait movement of mice, indicating

regeneration of injured nerve. “PE saline” refers to polyethylene tubing filled with saline solution and “PE collagen” refers to polyethylene tubing filled with native collagen fillers. “PAE saline” refers to poly(anhydride-ester) NGCs filled with saline. “PAE collagen” refers to poly (anhydride-ester) NGCs filled with native collagen fillers.

Despite the high standard error within each group, the trend is that NGCs filled with native collagen improve the recovery index when compared to NGCs filled with saline. This trend is in agreement with the literature in which NGCs filled with collagen-based hydrogels have improved functional recovery across 4 mm and 6 mm lesions of mouse sciatic nerve.[23] For a long gap nerve injury, NGCs primarily serve as a physical bridge during axon regeneration while fillers within the lumen of NGCs also actively promote the regeneration process.[25] A scaffold material provides pseudo-endoneurial structure that allows early ingrowth of neural and supporting cells.[25,28] The accelerated, regenerated growth of axons within filled NGCs appears to prevent the rapid loss of growth factors into the surrounding tissues whereas empty or unfilled NGCs lacks the supportive structures for regenerating axons and Schwann cells.[51] For saline-filled NGCs, PE NGCs did not produce a positive functional recovery, likely due to the prolonged denervation of quadriceps leading to muscular atrophy such that the body could not be supported during gait movements. For the PAE NGCs filled with saline, a positive functional recovery was observed.

Figure 10 represents two histological samples from an individual mouse in the PAE saline group that resulted in positive functional recovery. Although in Figure 9 PAE-saline group are statistically not significant ($p>0.05$) from other groups, evidence of axonal regeneration and remyelination of axons was evident while

samples from the rest of the group did not show much axonal regeneration or functional recovery.

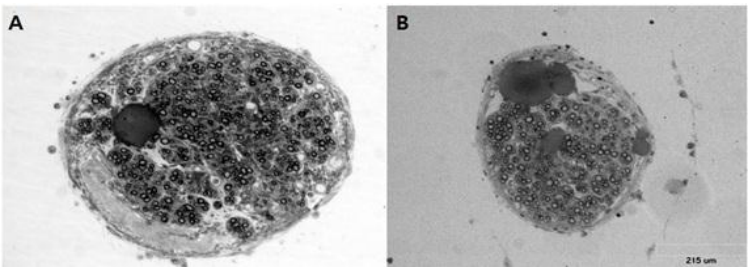

Figure 10. Representative samples from PAE-based NGCs filled with saline: (A) sample number 31 showing remyelination and (B) sample number 32 showing remyelination.

Figure 11 shows details of histological samples, where **Figure 11A** and **Figure 11B** (PE samples) have more scar tissue present within in the nerve and **Figure 10C** and **Figure 11D** (PAE samples) have less scar tissue.

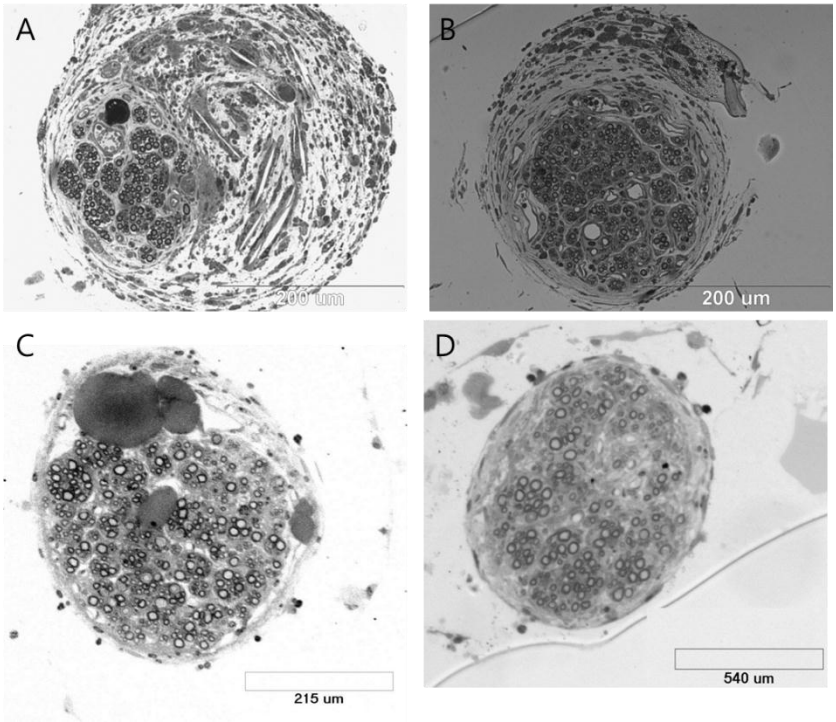

Figure 11. Histology of representative samples: (A) PE NGC filled with saline; (B) PE NGC filled with native collagen; (C) PAE NGC filled with saline; and (D) PAE NGC filled with native collagen.

One possible explanation behind the decreased scar tissue formation in PAE-treated samples is that the release of salicylic acid from the NGC during the course of regeneration decreases local inflammation. TNF-α is secreted by macrophages and

glial cells, such as Schwann cells in the peripheral nerve system.[52,53] The evidence is clear that TNF-α secreted from glia cells can inhibit neurite elongation and branching during development and regeneration.[54] Thus, the localized release of salicylic acid for the PAE NGCs may decrease the production of TNF-α secretion.[55-57] Similarly, Griffin et al. demonstrated that release of salicylic acid from PAE-based NGCs reduced secretion of TNF-α from macrophages *in vitro*[38].

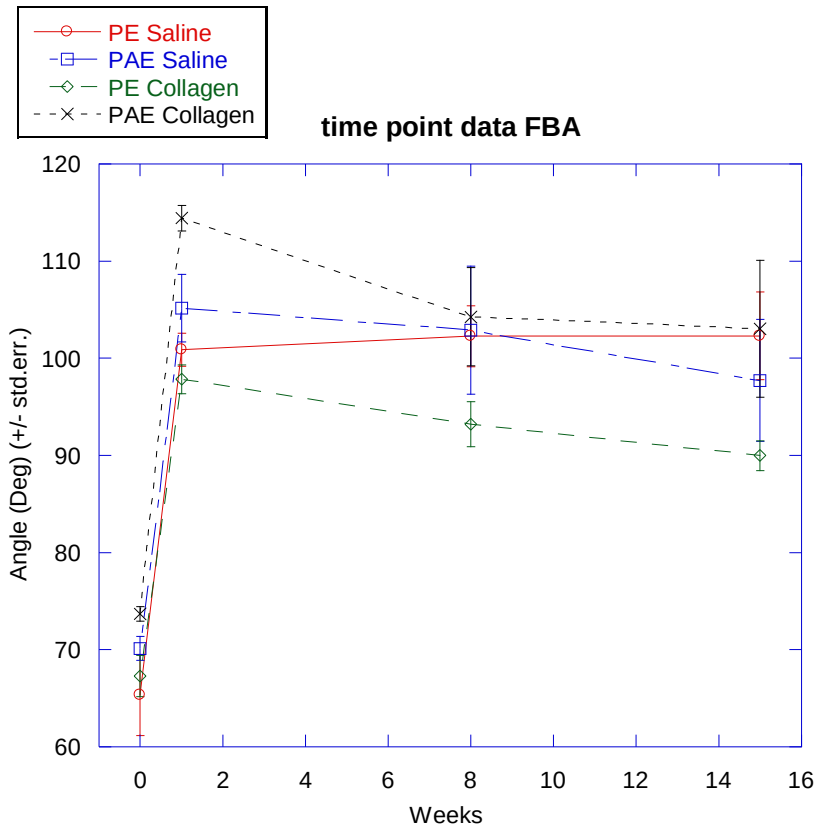

Figure 12. Foot base angle measurement at different time points.

Figure 12 depicts the FBA of mice at different time points. PE saline did not show any improvement at week 8, halfway through the *in vivo* study while other groups showed improvements. **Figure 12** also shows that for all groups other than PE saline during first 7 weeks of the study, greater improvement rates were observed in FBA than during the second 7 weeks, when functional improvement rates decreased slightly. As expected, NGCs filled with collagen displayed greater rates of functional

recovery, when compared to saline filled NGCs during the first 7 weeks of the study. All data in **Figure 12** was plotted as mean ± standard error.

Statistical analyses were run to examine the statistical significance of the data presented in **Figure 9**. **Table 1** summarizes the p-values.

Groups	p value
PAE Saline-PAE Collagen	**0.977975**
PE Collagen-PAE Collagen	**1**
PE Saline-PAE Collagen	**0.370689**
PE Collagen-PAE Saline	**0.965626**
PE Saline-PAE Saline	**0.638646**
PE Saline-PE Collagen	**0.221417**
Saline-Collagen	**0.049**
PE-PAE	**0.426**

Table 1. Summary of p-values for functional test: classical beam walk test

One-way ANOVA and two-way ANOVA gave p-values greater than 0.05, indicating that no statistical significance was observed between groups. Post-hoc Tukey's test was also run to compare each group. Tukey's test shows that for PE saline and PE collagen resulted p value of 0.04927. Based on this finding, PE saline and PE collagen are statistically different. This results from having double the sampling numbers (n=11) compared to sampling numbers for PAE saline (n=6) and PAE collagen (n=6). The statistical insignificance in the rest of the study may come from the limited sample size of test groups and unbalanced samples compared to the control group.

4.2. Functional recovery assessment: Pencil grip test

Figure 13 compares the functional recovery of mice treated with PE NGCs and PAE NGCs each filled with either saline or native collagen. All data in **Figure 13** was plotted as mean ± standard error. Higher functional recovery occurred with PE treated groups relative to the PAE-based NGCs. However, the pencil grip test measurement is

not as accurate as the classical beam walk test described in the previous section for two reasons.

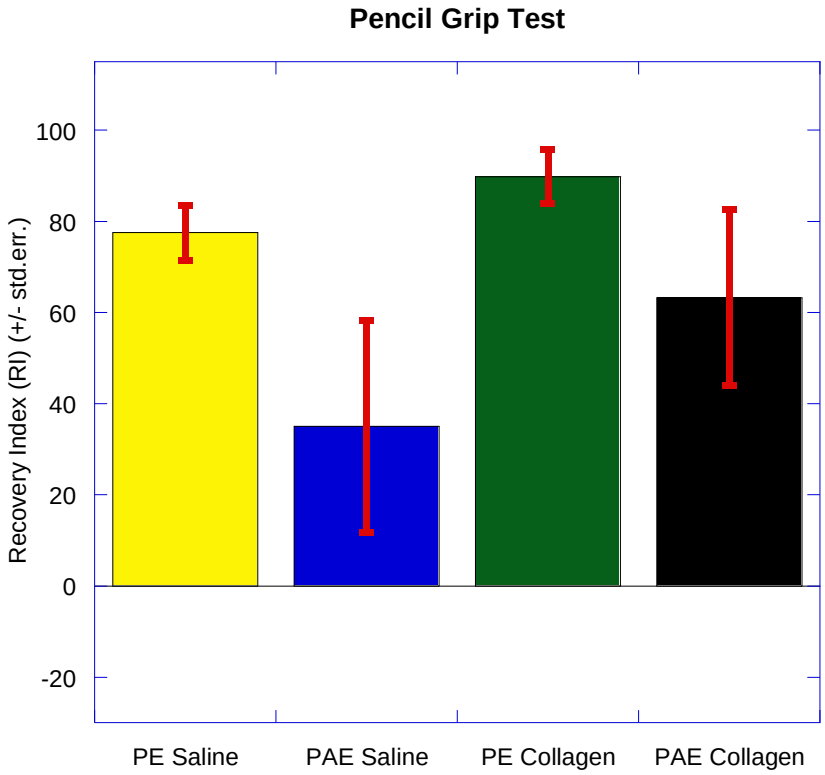

Figure 13. Pencil grip tests: Functional recovery of PLR measurements of different NGCs filled with saline and native collagen after 15 weeks post-surgery.

First, the pencil grip test measures an animal's reflex to extend the leg towards the pencil where it is held by its tail. Second, unlike the classical beam walk test, the animal does not support its body weight and may therefore rely on the force of gravity to extend the legs. The data in **Figure 13** appears to support high functional recovery for native collagen-filled PE NGC. Functional recovery in the PAE NGC treated groups was lower than PE NGC treated groups measurement but both groups follow the same trend: the native collagen filling improves functional recovery compared to saline-filled NGCs. Overall, the data in **Figure 13 shows that when NGCs are filled with collagen hydrogels, greater improvements were observed.**

Figure 14 depicts the pencil grip test results of mice at different time points. Only PE collagen showed greater improvement at week 8, halfway through the *in vivo* study, while other groups showed little improvements.

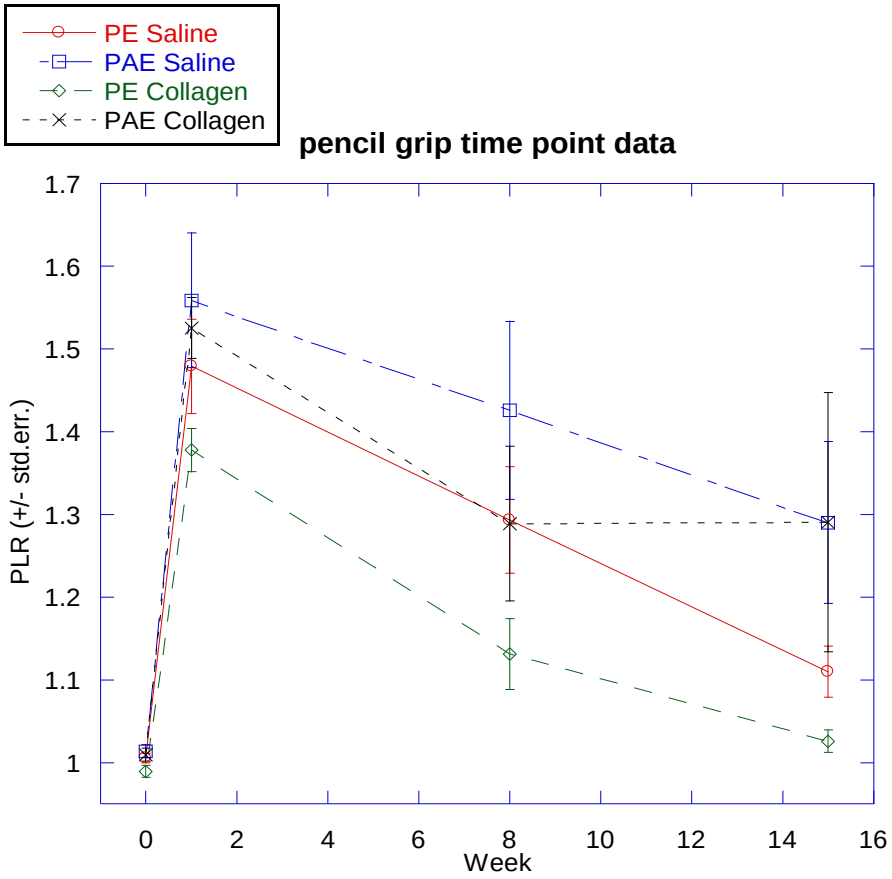

Figure 14. Pencil grip measurement at different time points.

Figure 14 also shows that during the first 8 weeks of the study, greater improvement rates were observed in FBA than in the second 8 weeks where functional improvement rates decreased slightly. Based on **Figure 14**, PE groups showed greater functional recovery compared to PAE groups as the PLR values restored closer to 1 while PLR value of PAE groups were at 1.3. As expected, NGCs filled with collagen displayed greater rate of functional recovery, when compared to saline filled NGCs during first 8 weeks of the study. All data in **Figure 14** was plotted as mean ± standard error.

Statistical studies were run to examine the statistical significance of the data. **Table 2** summarizes the p-values.

Groups	p values
PAE Saline-PAE Collagen	**0.590755**
PE Collagen-PAE Collagen	**0.638125**
PE Saline-PAE Collagen	**0.916507**
PE Collagen-PAE Saline	**0.096875**
PE Saline-PAE Saline	**0.253487**
PE Saline-PE Collagen	**0.945657**
Saline-Collagen	**0.21264**
PE-PAE	**0.03991**

Table 2. Summary of p-values for functional test: Pencil grip test

Studies show that NGC materials have effects on pencil grip based functional recovery as shown in **Figure 13**. Both one-way and two-way ANOVA tests showed a lack of statistical significance for filler types, which may come from the limited and unbalanced sample sizes of test groups compared to the control group.

4.3. g-Ratio analysis

Figure 15 shows that all NGCs regenerated axons with proper myelin thickness as determined by the g-ratio. All data in **Figure 15** was plotted as mean ± standard error. In normal nerves, a g-ratio between 0.6 and 0.7 is observed for rats and mice.[50,58] The measurements for each group were analyzed using representative samples that showed regeneration of axons. Statistical studies were run to examine the significance of the data. **Table 3** summarizes the p-values. As seen in **Figure 15**, the groups do not show much statistical significance due to small and unbalanced sample sizes. For all groups, regenerated nerves exhibited proper myelination as indicated by average g-ratio values within the normal physiological range.

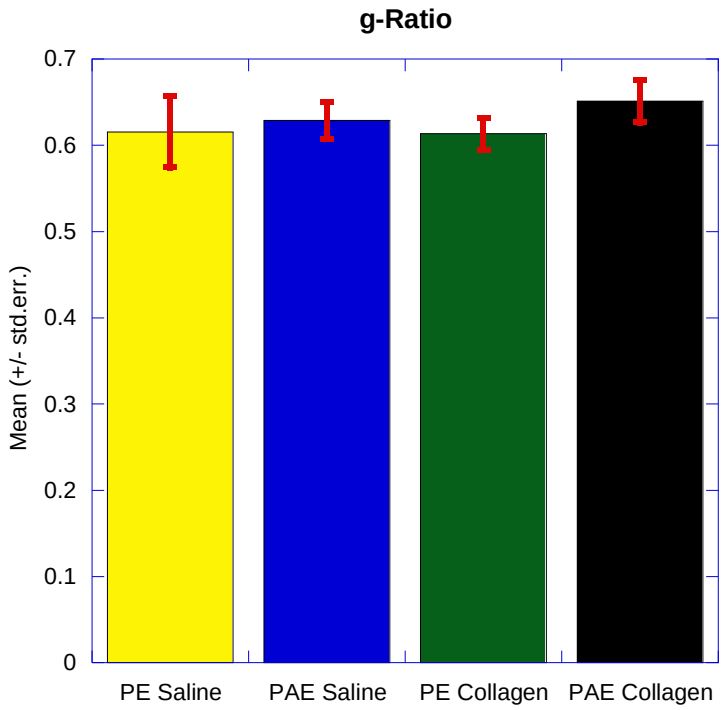

Figure 15. g-Ratio of NGCs.

Groups	p values
PAE Saline-PAE Collaen	0.9523
PE Collagen-PAE Collaen	0.718446
PE Saline-PAE Collaen	0.789578
PE Collagen-PAE Saline	0.984421
PE Saline-PAE Saline	0.991262
PE Saline-PE Collagen	1
PE-PAE	0.3069
Saline-Collagen	0.5709

Table 3. Summary of p-values for g-ratio.

4.4. Degree of regeneration

Figure 16 displays the degree of nerve regeneration, defined by area of regenerated nerve over whole nerve, using different NGCs and fillers. While no significant difference ($p>0.05$) is observed between groups with saline and native collagen, a significant difference is observed between the different types of NGCs ($p<0.05$). PAE-based NGCs promoted greater regeneration than PE NGCs regardless of whether they were filled with saline or native collagen.

NGCs should serve as a physical barrier to prevent infiltration of fibroblasts that may interrupt nerve connection, yet fibroblasts may enter from the proximal end of the nerve and deposit at the injury site. Inflammatory responses are governed by many transcription factors such as NF-κB (nuclear factor-κB) that are activated upon cell injury.[59] NF-κB can be inhibited by NSAIDs and studies have shown that aspirin can indirectly inhibit the activity of NF-κB by blocking enzymes and also irreversibly inactivating cyclooxygenase (COX) isoforms leading to reduced inflammation and scar tissue formation.[59] During the course of regeneration, the release of salicylic acid from the PAE NGCs likely prevent scar tissues formation by inhibiting the COX-2 pathway, thus allowing more nerves to regenerate while the lumen of PE NGCs were filled with fibroblast scar tissue. This result is confirmed in **Figure 11** where PE NGC filled with saline and native collagen generated excessive scar tissue while PAE NGC showed less fibroblast derived scar tissue within the nerve. Statistical studies were performed and summarized in **Table 4.**

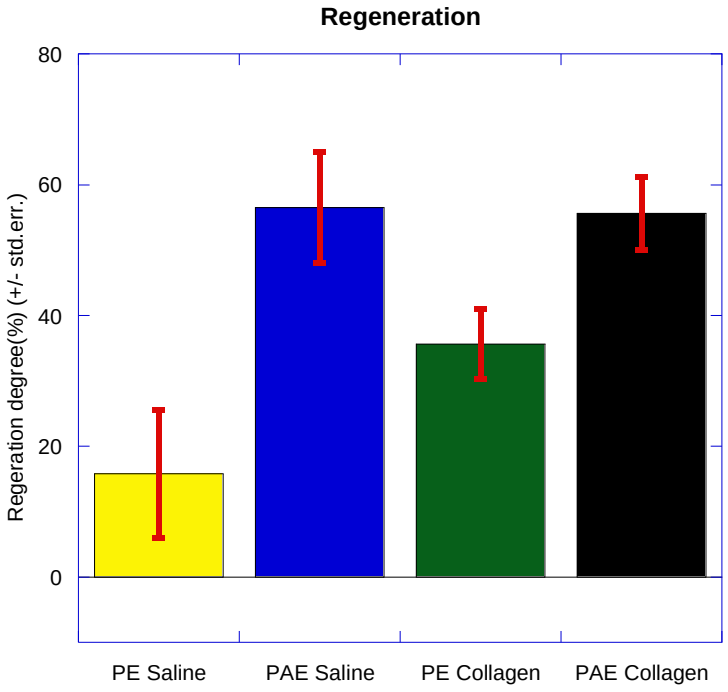

Figure 16. Nerve regeneration degree.

Groups	p values
PAE Saline-PAE Collagen	**0.999784**
PE Collagen-PAE Collagen	**0.254192**
PE Saline-PAE Collagen	**0.019812**
PE Collagen-PAE Saline	**0.22547**
PE Saline-PAE Saline	**0.017552**
PE Saline-PE Collagen	**0.259224**
PE-PAE	**0.003166**
Saline-Collagen	**0.195339**

Table 4. Summary of p-values for nerve regeneration.

Overall two-way ANOVA showed p-values less than 0.05 for NGC types. Pairwise comparison of PE saline versus PAE collagen and PE saline versus PAE saline show that they are statistically different ($p<0.05$). Overall, more regeneration was observed when PAE NGCs were used compared to groups that were treated with PE NGCs. Compared to functional recovery assessment, nerve regeneration resulted in statistically significant data arising from having greater number of regenerated axons within the nerve whereas poorly regenerated nerve contained far less regenerated axons.

5. CONCLUSIONS

PAE NGCs were implanted in mice to evaluate their potential to aid peripheral nerve regeneration following injury. This research studied the gait behavior of the animals and quantified the degree of femoral nerve regeneration. When filled with collagen, PAE-based NGCs performed on par or slightly better than PE-based NGCs filled with collagen. In addition, PAE-based NGCs function as local drug delivery vehicle by degrading to salicylic acid to reduce inflammation associated with nerve and surrounding tissue injury as seen with less scar tissue on histology. For both PE and PAE NGCs, native collagen provided a favorable environment for axons to regenerate. Controlled release of salicylic acid from NGCs may also aid in the regeneration process by inhibiting TNF-α that inhibits neurite outgrowth. In brief,

PAE-based NGC demonstrated potential for repairing peripheral nerve injury due to its fabrication technique and drug-eluting property.

6. APPENDIX

6.1. Current and future work

Ongoing studies include *in vitro* optimization of concentration-dependent TNF-α inhibition from macrophages using PAE-based NGCs. Future *in vivo* studies will include an increased number of samples per experimental group to obtain statistically significant data. [53] Both *in vitro* and *in vivo* experiments will be carried out to determine the effect of controlled release of salicylic acid from PAE on neurite outgrowth and ultimately, peripheral nerve repair.[60-64] An *in vivo* study will be used to quantify the reduced inflammation during nerve regeneration. By measuring mRNA levels of TNF-α and IFN-γ using reverse transcription polymerase chain reaction (RT-PCR) during nerve regeneration, this study may reveal the effects of controlled released of salicylic acid during degradation of the NGC.[53] The next generation of salicylic acid-based NGCs will be fabricated using different blends of other biodegradable polymers and tested both *in vitro* and *in vivo*. Lastly, PAE-based NGCs will be incorporated with microspheres encapsulating various growth factors to promote nerve regeneration through prolonged delivery of growth factors. Studies have shown that prolonged delivery of growth factors increases the regeneration of injured nerves.[23] Designing NGCs that can achieve prolonged delivery of growth factors would eliminate the need for continuous injection or infusion of neurotropic factors.

7. REFERENCES

1 Noble, J. M., Catherine A. MSc; Prasad, Vannemreddy S. S. V. MCh; Midha, Rajiv MD, MSc, FRCS(C). Analysis of Upper and Lower Extremity Peripheral Nerve Injuries in a Population of Patients with Multiple Injuries. *The Journal of Trauma: Injury, Infection, and Critical Care* **45**, 116-122 (1998).

2 Kingham, P. J. & Terenghi, G. Bioengineered nerve regeneration and muscle reinnervation. *J Anat* **209**, 511-526, doi:JOA623 [pii]
10.1111/j.1469-7580.2006.00623.x (2006).

3 Wiberg, M. & Terenghi, G. Will it be possible to produce peripheral nerves? *Surg Technol Int* **11**, 303-310 (2003).

4 Lundborg, G. & Rosen, B. Hand function after nerve repair. *Acta Physiol (Oxf)* **189**, 207-217, doi:APS1653 [pii]
10.1111/j.1748-1716.2006.01653.x (2007).

5 Robinson, L. R. Traumatic injury to peripheral nerves. *Muscle & Nerve* **23**, 863-873 (2000).

6 Smith, B. E. Anatomy and histology of peripheral nerve. *Handbook of Clinical Neurophysiology* **7**, 3-22 (2006).

7 Brown, A. Axonal transport of membranous and nonmembranous cargoes: a unified perspective. *J Cell Biol* **160**, 817-821, doi:10.1083/jcb.200212017
jcb.200212017 [pii] (2003).

8 Jiang, X., Lim, S. H., Mao, H. Q. & Chew, S. Y. Current applications and future perspectives of artificial nerve conduits. *Exp Neurol* **223**, 86-101, doi:S0014-4886(09)00382-3 [pii]
10.1016/j.expneurol.2009.09.009 (2010).

9 Johnson, E. O., Zoubos, A. B. & Soucacos, P. N. Regeneration and repair of peripheral nerves. *Injury* **36 Suppl 4**, S24-29, doi:S0020-1383(05)00420-1 [pii]
10.1016/j.injury.2005.10.012 (2005).

10 Stoll, G. & Muller, H. W. Nerve injury, axonal degeneration and neural regeneration: basic insights. *Brain Pathol* **9**, 313-325 (1999).

11 Stoll, G., Jander, S. & Myers, R. R. Degeneration and regeneration of the peripheral nervous system: from Augustus Waller's observations to neuroinflammation. *J Peripher Nerv Syst* **7**, 13-27 (2002).

12 Gaudet, A. D., Popovich, P. G. & Ramer, M. S. Wallerian degeneration: gaining perspective on inflammatory events after peripheral nerve injury. *J Neuroinflammation* **8**, 110, doi:1742-2094-8-110 [pii]
10.1186/1742-2094-8-110 (2011).

13 Seckel, B. R. Enhancement of peripheral nerve regeneration. *Muscle Nerve* **13**, 785-800, doi:10.1002/mus.880130904 (1990).

14 Hirata, K. & Kawabuchi, M. Myelin phagocytosis by macrophages and nonmacrophages during Wallerian degeneration. *Microsc Res Tech* **57**, 541-547, doi:10.1002/jemt.10108 (2002).

15 Fenrich, K. & Gordon, T. Canadian Association of Neuroscience review: axonal regeneration in the peripheral and central nervous systems--current issues and advances. *Can J Neurol Sci* **31**, 142-156 (2004).

16 Liu, H. M. The role of extracellular matrix in peripheral nerve regeneration: a wound chamber study. *Acta Neuropathol* **83**, 469-474 (1992).

17 Ceballos, D. *et al.* Magnetically aligned collagen gel filling a collagen nerve guide improves peripheral nerve regeneration. *Exp Neurol* **158**, 290-300, doi:10.1006/exnr.1999.7111
S0014-4886(99)97111-X [pii] (1999).
18 Evans, G. R. Peripheral nerve injury: a review and approach to tissue engineered constructs. *Anat Rec* **263**, 396-404, doi:10.1002/ar.1120 [pii] (2001).
19 Lee, S. K. & Wolfe, S. W. Peripheral nerve injury and repair. *J Am Acad Orthop Surg* **8**, 243-252 (2000).
20 Yucel, D., Kose, G. T. & Hasirci, V. Polyester based nerve guidance conduit design. *Biomaterials* **31**, 1596-1603, doi:S0142-9612(09)01225-3 [pii]
10.1016/j.biomaterials.2009.11.013 (2010).
21 Agnew, S. P. & Dumanian, G. A. Technical use of synthetic conduits for nerve repair. *J Hand Surg Am* **35**, 838-841, doi:S0363-5023(10)00253-4 [pii]
10.1016/j.jhsa.2010.02.025 (2010).
22 Johnson, E. O. & Soucacos, P. N. Nerve repair: experimental and clinical evaluation of biodegradable artificial nerve guides. *Injury* **39 Suppl 3**, S30-36, doi:S0020-1383(08)00257-X [pii]
10.1016/j.injury.2008.05.018 (2008).
23 Deumens, R. *et al.* Repairing injured peripheral nerves: Bridging the gap. *Prog Neurobiol* **92**, 245-276, doi:S0301-0082(10)00172-3 [pii]
10.1016/j.pneurobio.2010.10.002 (2010).
24 Lewin-Kowalik, J., Marcol, W., Kotulska, K., Mandera, M. & Klimczak, A. Prevention and management of painful neuroma. *Neurol Med Chir (Tokyo)* **46**, 62-67; discussion 67-68, doi:JST.JSTAGE/nmc/46.62 [pii] (2006).
25 Gu, X., Ding, F., Yang, Y. & Liu, J. Construction of tissue engineered nerve grafts and their application in peripheral nerve regeneration. *Prog Neurobiol* **93**, 204-230, doi:S0301-0082(10)00193-0 [pii]
10.1016/j.pneurobio.2010.11.002 (2011).
26 Cao, J. *et al.* The use of laminin modified linear ordered collagen scaffolds loaded with laminin-binding ciliary neurotrophic factor for sciatic nerve regeneration in rats. *Biomaterials* **32**, 3939-3948, doi:S0142-9612(11)00172-4 [pii]
10.1016/j.biomaterials.2011.02.020 (2011).
27 Cai, S. W. a. L. Polymers for Fabricating Nerve Conduits. *International Journal of Polymer Science* **2010** (2010).
28 de Ruiter, G. C., Malessy, M. J., Yaszemski, M. J., Windebank, A. J. & Spinner, R. J. Designing ideal conduits for peripheral nerve repair. *Neurosurg Focus* **26**, E5, doi:10.3171/FOC.2009.26.2.E5 (2009).
29 Griffin, J., Carbone, A., Delgado-Rivera, R., Meiners, S. & Uhrich, K. E. Design and evaluation of novel polyanhydride blends as nerve guidance conduits. *Acta Biomater* **6**, 1917-1924, doi:S1742-7061(09)00519-4 [pii]
10.1016/j.actbio.2009.11.023 (2010).
30 Zhao, Q., Dahlin, L. B., Kanje, M. & Lundborg, G. Repair of the transected rat sciatic nerve: matrix formation within implanted silicone tubes. *Restor Neurol Neurosci* **5**, 197-204, doi:124KQ07666093834 [pii]
10.3233/RNN-1993-5304 (1993).
31 Madison, R. D., da Silva, C., Dikkes, P., Sidman, R. L. & Chiu, T. H. Peripheral nerve regeneration with entubulation repair: comparison of biodegradeable nerve guides versus polyethylene tubes and the effects of a

laminin-containing gel. *Exp Neurol* **95**, 378-390, doi:0014-4886(87)90146-4 [pii] (1987).

32 Bergsma, E. J., Rozema, F. R., Bos, R. R. & de Bruijn, W. C. Foreign body reactions to resorbable poly(L-lactide) bone plates and screws used for the fixation of unstable zygomatic fractures. *J Oral Maxillofac Surg* **51**, 666-670, doi:S0278239193000953 [pii] (1993).

33 Li, L. C., Deng, J. & Stephens, D. Polyanhydride implant for antibiotic delivery--from the bench to the clinic. *Adv Drug Deliv Rev* **54**, 963-986, doi:S0169409X02000534 [pii] (2002).

34 Uhrich, K. E., Cannizzaro, S. M., Langer, R. S. & Shakesheff, K. M. Polymeric systems for controlled drug release. *Chemical Reviews* **99**, 3181-3198 (1999).

35 Erdmann, L. & Uhrich, K. E. Synthesis and degradation characteristics of salicylic acid-derived poly(anhydride-esters). *Biomaterials* **21**, 1941-1946, doi:S0142-9612(00)00073-9 [pii] (2000).

36 Whitaker-Brothers, K. & Uhrich, K. Poly(anhydride-ester) fibers: role of copolymer composition on hydrolytic degradation and mechanical properties. *J Biomed Mater Res A* **70**, 309-318, doi:10.1002/jbm.a.30083 (2004).

37 Almudena Prudencio, R. C. S., and Kathryn E. Uhrich. Effect of Linker Structure on Salicylic Acid-Derived Poly(anhydride-esters). *Macromolecules* **38**, 6895-6901 (2005).

38 Griffin, J. *The design and fabrication of novel polyanhydride blend scaffolds for peripheral nerve repair* Doctor of Philosophy thesis, Rutgers University, (2011).

39 Schmeltzer, R. C., Schmalenberg, K. E. & Uhrich, K. E. Synthesis and cytotoxicity of salicylate-based poly(anhydride esters). *Biomacromolecules* **6**, 359-367, doi:10.1021/bm049544+ (2005).

40 Wu, P. & Grainger, D. W. Drug/device combinations for local drug therapies and infection prophylaxis. *Biomaterials* **27**, 2450-2467, doi:S0142-9612(05)01057-4 [pii]
10.1016/j.biomaterials.2005.11.031 (2006).

41 Labrador, R. O., Buti, M. & Navarro, X. Influence of collagen and laminin gels concentration on nerve regeneration after resection and tube repair. *Exp Neurol* **149**, 243-252, doi:S0014-4886(97)96650-4 [pii]
10.1006/exnr.1997.6650 (1998).

42 Suzuki, K. *et al.* Histologic and electrophysiological study of nerve regeneration using a polyglycolic acid-collagen nerve conduit filled with collagen sponge in canine model. *Urology* **74**, 958-963, doi:S0090-4295(09)00328-8 [pii]
10.1016/j.urology.2009.02.057 (2009).

43 Schmeltzer, R. C., Anastasiou, T. J. & Uhrich, K. E. Optimized synthesis of salicylate-based poly(anhydride-esters). *Polym Bull* **49**, 441-448 (2003).

44 Masand, S. N., Perron, I. J., Schachner, M. & Shreiber, D. I. Neural cell type-specific responses to glycomimetic functionalized collagen. *Biomaterials* **33**, 790-797, doi:S0142-9612(11)01216-6 [pii]
10.1016/j.biomaterials.2011.10.013 (2012).

45 Shreiber, D. I., Barocas, V. H. & Tranquillo, R. T. Temporal variations in cell migration and traction during fibroblast-mediated gel compaction. *Biophys J* **84**, 4102-4114, doi:S0006-3495(03)75135-2 [pii]
10.1016/S0006-3495(03)75135-2 (2003).

46 Irintchev, A., Simova, O., Eberhardt, K. A., Morellini, F. & Schachner, M. Impacts of lesion severity and tyrosine kinase receptor B deficiency on functional outcome of femoral nerve injury assessed by a novel single-frame motion analysis in mice. *Eur J Neurosci* **22**, 802-808, doi:EJN4274 [pii]
10.1111/j.1460-9568.2005.04274.x (2005).
47 Mehanna, A. *et al.* Polysialic acid glycomimetics promote myelination and functional recovery after peripheral nerve injury in mice. *Brain* **132**, 1449-1462, doi:awp128 [pii]
10.1093/brain/awp128 (2009).
48 Smith, B. E. Chapter 1 Anatomy and histology of peripheral nerve. *Handbook of Clinical Neurophysiology* **7**, 19 (2006).
49 Chomiak, T. & Hu, B. What is the optimal value of the g-ratio for myelinated fibers in the rat CNS? A theoretical approach. *PLoS One* **4**, e7754, doi:10.1371/journal.pone.0007754 (2009).
50 Guy, J., Ellis, E. A., Kelley, K. & Hope, G. M. Spectra of G ratio, myelin sheath thickness, and axon and fiber diameter in the guinea pig optic nerve. *J Comp Neurol* **287**, 446-454, doi:10.1002/cne.902870404 (1989).
51 Pabari, A., Yang, S. Y., Mosahebi, A. & Seifalian, A. M. Recent advances in artificial nerve conduit design: strategies for the delivery of luminal fillers. *J Control Release* **156**, 2-10, doi:S0168-3659(11)00478-0 [pii]
10.1016/j.jconrel.2011.07.001 (2011).
52 Wagner, R. & Myers, R. R. Schwann cells produce tumor necrosis factor alpha: expression in injured and non-injured nerves. *Neuroscience* **73**, 625-629, doi:0306-4522(96)00127-3 [pii] (1996).
53 Taskinen, H. S. *et al.* Peripheral nerve injury induces endoneurial expression of IFN-gamma, IL-10 and TNF-alpha mRNA. *J Neuroimmunol* **102**, 17-25, doi:S0165-5728(99)00154-X [pii] (2000).
54 Neumann, H. *et al.* Tumor necrosis factor inhibits neurite outgrowth and branching of hippocampal neurons by a rho-dependent mechanism. *J Neurosci* **22**, 854-862, doi:22/3/854 [pii] (2002).
55 An, Y., Liu, K., Zhou, Y. & Liu, B. Salicylate inhibits macrophage-secreted factors induced adipocyte inflammation and changes of adipokines in 3T3-L1 adipocytes. *Inflammation* **32**, 296-303, doi:10.1007/s10753-009-9135-1 (2009).
56 Zu, L. *et al.* Salicylate blocks lipolytic actions of tumor necrosis factor-alpha in primary rat adipocytes. *Mol Pharmacol* **73**, 215-223, doi:mol.107.039479 [pii]
10.1124/mol.107.039479 (2008).
57 Vittimberga, F. J., Jr., McDade, T. P., Perugini, R. A. & Callery, M. P. Sodium salicylate inhibits macrophage TNF-alpha production and alters MAPK activation. *J Surg Res* **84**, 143-149, doi:10.1006/jsre.1999.5630
S0022-4804(99)95630-5 [pii] (1999).
58 Fansa, H., Schneider, W., Wolf, G. & Keilhoff, G. Influence of insulin-like growth factor-I (IGF-I) on nerve autografts and tissue-engineered nerve grafts. *Muscle Nerve* **26**, 87-93, doi:10.1002/mus.10165 (2002).
59 Roseborough, I. E., Grevious, M. A. & Lee, R. C. Prevention and treatment of excessive dermal scarring. *J Natl Med Assoc* **96**, 108-116 (2004).
60 Desbarats, J. *et al.* Fas engagement induces neurite growth through ERK activation and p35 upregulation. *Nat Cell Biol* **5**, 118-125, doi:10.1038/ncb916
ncb916 [pii] (2003).

61 Namgung, U. *et al.* Activation of cyclin-dependent kinase 5 is involved in axonal regeneration. *Mol Cell Neurosci* **25**, 422-432, doi:10.1016/j.mcn.2003.11.005
S1044743103003592 [pii] (2004).

62 Nikolic, M., Dudek, H., Kwon, Y. T., Ramos, Y. F. & Tsai, L. H. The cdk5/p35 kinase is essential for neurite outgrowth during neuronal differentiation. *Genes Dev* **10**, 816-825 (1996).

63 Subbanna, P. K., Prasanna, C. G., Gunale, B. K. & Tyagi, M. G. Acetyl salicylic acid augments functional recovery following sciatic nerve crush in mice. *J Brachial Plex Peripher Nerve Inj* **2**, 3, doi:1749-7221-2-3 [pii]
10.1186/1749-7221-2-3 (2007).

64 Vartiainen, N., Keksa-Goldsteine, V., Goldsteins, G. & Koistinaho, J. Aspirin provides cyclin-dependent kinase 5-dependent protection against subsequent hypoxia/reoxygenation damage in culture. *J Neurochem* **82**, 329-335 (2002).